Published by Avanti Publishers

Global Journal of Earth Science and Engineering

ISSN (online): 2409-5710

Crustal and Lithospheric Variations along the Western Passive Continental Margin of the Indian Peninsula

Muthyala Prasad[1,2] and Chandra P. Dubey[1,*]

[1]Solid Earth Research Group, National Centre for Earth Science Studies, Thiruvananthapuram, Kerala 695011, India

[2]Department of Marine Geology and Geophysics, Cochin University of Science and Technology (CUSAT), Kochi 682022, India

ARTICLE INFO

Article Type: Research Article

Keywords:
Uncertainties
2-D modeling
Spectral analysis
The western ghats

Timeline:
Received: May 30, 2023
Accepted: November 07, 2023
Published: December 14, 2023

Citation: Prasad M, Dubey CP. Crustal and lithospheric variations along the western passive continental margin of the Indian Peninsula. Glob J Earth Sci Eng. 2023; 10: 1-13.

DOI: https://doi.org/10.15377/2409-5710.2023.10.1

ABSTRACT

The western passive continental margin (WPCM) of the Indian Peninsula is one of the world's largest and most remarkable escarpments, signifying a boundary between oceanic and continental lithospheres. It traverses distinct lithological units, majorly the SGT, WDC, and DVP, each characterized by distinct geological structures, geochronological histories, and petro-physical properties. Despite numerous research efforts, the exact mechanisms governing the WPCM evolution and its developmental connections remain unclear due to limited data and significant uncertainties. In our study, we meticulously analyzed global and local models, focusing on the Western Ghats (WG), to examine crust and lithosphere thickness. Our analysis revealed significant uncertainties in crustal and lithospheric variations, with a maximum difference of 10.68% in crust thickness and 20.04% in lithospheric thickness across different major lithological formations in the WG. These differences can have a substantial impact on the geodynamic analysis of lithospheric structures and tectonic evolution. Additionally, we developed a 2-D lithospheric density model over the WG, crossing the major geological units, which delineates the crust and lithospheric structure between the eastern and western sides of the escarpment. Our results, in conjunction with geomorphological data, suggest that the WPCM's thick lithosphere with elevated topography illustrates a continuous upwarp, supported by flexural compensation of uplifted terrain. The movement of the Indian plate, primarily in the N-S and NW-SE directions, subsequently modified the entire escarpment. This model offers insights into the evolution of the WPCM and potentially contributes to the formation of the NE-SW fault in the southern part of the South Indian Shield, with potential implications for the Palghat gap.

*Corresponding Author
Email: p.dubey48@gmail.com
Tel: +(91)-628 297 2507

1. Introduction

The origin and evolution of continents represent one of the greatest challenges in the field of Earth Science research today. Unraveling the history, internal dynamics, and evolution of the lithosphere, both in continental and oceanic settings, can provide insights into how the Earth's crust formed, the inception of plate tectonics, and the development of habitable continents. In the modern Earth, this knowledge enhances our understanding of the nature and evolution of tectonic plates [1], The present-day configuration of the Western passive continental margin of India is a consequence of its extensive and intricate tectonic history.

The Western Ghats, known as the Sahyadri in its present-day configuration, ranks among the world's most spectacular and extensive escarpments, alongside those found in Australia, Brazil, and the South African passive margins. This long-uplifted topographical scarp (Fig. **1b**) represents a prominent geomorphic feature. It encompasses uneven topography, deep valleys, numerous impressive waterfalls, dense forests, a complex geological history, extensive volcanic activity, and various structures and petro-physical properties [2]. It stretches approximately 1600 kilometers in a nearly straight line, running in a north-northwest to south-southeast direction. The study area, with an average elevation of 1200 meters, traverses across six states: i) Gujarat ii) Maharashtra iii) Goa iv) Karnataka v) Kerala, and vi) Tamil Nadu. The maximum elevation reaches 2500 meters, and the escarpment is aligned roughly parallel to the west coastal region (Arabian Sea) of Peninsular India. Along the Western Ghats, there is only one significant low-elevation break known as the Palghat Gap. It spans approximately 30 kilometers in width, extending from the northern region of Gujarat to Kanyakumari.

The evolution of the topographic scarp in the Western Ghats has been studied extensively, with recognized perspectives from various fields including geomorphological, geochemical, geological, and geophysical studies. The most popular explanations are marginal rift flank uplift [3-5], mantle plume-related drifting [6, 7], magmatic under-plating [8, 9], lithospheric delamination [10], isostatic compensation [11, 12], increasing tectonic processes and denudation rates [13-18], and flexural adjustment [19-21]. As per [22], the causes of upliftment can be categorized into three distinct ways: (i) Density reduction, either mechanically or thermal processes, in response to isostatic adjustments. (ii) Crustal buoyancy, attributed to an increase in lithospheric thickness, and (iii) Plastic necking, resulting from stretching and uneven denudation of lithosphere on both sides of the scarp.

Recent studies have put forth various hypotheses regarding the formation of the Western Ghats. These include active rifting and extensional tectonics [23], igneous underplating [24], flexural isostatic adjustment of uplifted topography, later modified by tectonic and denudation processes [25], crust and mantle interactions during tectonic-magmatism associated with the Deccan volcanic provinces [26], and multistage rifting episodes [27-29].

While numerous studies, as mentioned earlier, have proposed multiple hypotheses and theories to comprehend the evolution of the WG and its connection with the expansion of the Western Passive Continental Margin (WPCM), a conclusive explanation for the evolution of the WG remains elusive [30, 31]. This is due to the region's diverse lithological variations, complex interactions between the crust and mantle, the presence of the Palghat gap interrupting the topography, and the exposure of lower crustal rocks in the entire Southern Granulite Terrain (SGT) [32]. Here, we conducted a comparative analysis of various models of crustal and lithospheric thickness in the study region. We aim to evaluate the effectiveness of different modeling techniques and the influence of varying data sources on these models' quality. Additionally, we have developed 2-D lithospheric density models along the Western Ghats (WG) using satellite-derived EGM 2008 gravity data. These models have been constrained by previous results, aiming to enhance our understanding of the factors contributing to the evolution of the WG by enabling us to decipher the underlying crust and lithospheric structure.

2. Geology and Tectonic Setting

The Western Ghats are a highly topographic region in India, after the Himalayan Mountain building. The present WPCM of India and the surrounding regions formed through several stages of rifting episodes that occurred before the break-up Gondwana supercontinent around 180 Ma [33, 34]. Geological history indicates that during the early Jurassic period, the Gondwana supercontinent started to divide into two major landmasses: 1)

West Gondwana and 2) East Gondwana, as a result of continental drift. The West Gondwana is comprised of South America and Africa, which consists of a mosaic of Archean/Paleoproterozoic cratons and Neo-Proterozoic to Cambrian Pan-African orogenic systems [34-36]. On the other hand, the East Gondwanaland drifted south-south easterly relative to Africa in the Late Jurassic (170-120 Ma) constituted by India, Madagascar, Seychelles, Sri Lanka, Australia, and East Antarctica. Furthermore, within the West Gondwana, India and Madagascar began drifting away from Antarctica-Australia at approximately 140 Ma [37], and the dispersal process continued. [38] suggested that this could be attributed to thermo-mechanical interactions between these two continental lithospheric fragments. Later, at approximately 90 Ma, the India-Seychelles landmasses began to rift rapidly, moving northward and eventually separated from Madagascar due to the activity of the Marion plume [39] (Reeves, 2014 and references therein). At approximately 65 Ma, the Deccan flood basalts erupted as a result of the reunion plume hotspot activity, leading to the separation of the India-Seychelles continental blocks [40]. In general, continental lithospheric plate rifting and break-up are often associated with mantle plume activity. Consequently, many researchers believe that these two major rifting events strongly influenced the evolution and enlargement of the WPCM.

Based on geological formations, the entire Western Ghats region (Fig. **1a**) is divided into three parts: Northern, Middle, and Southern. The northern part, extending from latitude 16° to 20° N, is predominantly occupied by the Deccan Volcanic Provinces (DVP) and is commonly referred to as the Konkan coast. The Deccan Traps region is primarily characterized by thick sequences of volcanic lava flows, approximately 2 kilometers in thickness, concealing Mesozoic sediments and the remnants of Deccan volcanism beneath this zone [41]. The middle zone, situated between latitudes 12° to 16° N, is characterized by Precambrian volcano-sedimentary sequences. The Dharwar Craton in Peninsular India is one of the oldest continental Archean crusts, primarily composed of tonalite-trondhjemite gneisses and granites [42]. These rocks range from ~3600-2500 Ma and overlie the basement complex gneisses. Furthermore, the Dharwar Craton has been subdivided into two tectonic blocks: the Western Dharwar Craton (WDC) and the Eastern Dharwar Craton, based on differences in age, deformation, and tectonic history. The southern part, known as the Malabar Coast (latitude extending from 8° to 12° N), consists of high-grade granulite rocks found within the Southern Granulite Terrain (SGT). This highly metamorphosed SGT represents one of the world's most deeply exposed Precambrian continental crusts, which underwent deformation approximately 3500-550 Ma [43].

3. Crust and Lithospheric Variations

Understanding crust and lithospheric variations is crucial for comprehending the internal structure and geodynamic evolution of tectonic plates, as well as the formation of elevated surface topography. Global studies on crust and lithospheric thickness have revealed significant variability like the Earth's, comprising the crust and upper mantle, across different tectonic and lithological regions. In some locations, this boundary is well-defined, while in most others, it exhibits a diffused nature [44]. Crust and lithospheric thickness have been estimated using various geophysical methods over the past two decades in the Western Ghats and surrounding areas. In this region, several studies, either in part or as a whole, have examined the estimated crust and lithospheric thickness. These investigations have been conducted by various researchers using different geophysical methods, which are explained below.

3.1. Crust

From gravity studies, crustal thickness following range: SGT (35-44 km), EDC (32-38 km), WDC (40-52 km), DVP (30-50 km), and along the WPCM (38-53 km); [25, 45-49]. Various seismic and receiver function analyses: SGT (36-46 km), EDC (31-38 km), WDC (40-60 km), DVP (30-54 km), and along the WPCM (37-45 km); [26, 29, 50-56].

3.2. LAB

The estimated LAB depths by different techniques (Surface wave analysis, receiver functions, Magnetotelluric data, gravity, and geoid anomaly) made by various authors is as follows: SGT (120-185 km), EDC (70-185 km), WDC (100-200 km), DVP (95-120 km), and beneath the WPCM (~160 km); [57-64].

4. Data Utilization

Geophysical potential field methods, particularly the gravity method, measure the Earth's gravitational field as influenced by surface and subsurface rocks, structures, and physical properties such as density distributions. Satellite-derived global gravity models have limitations because they do not represent short wavelengths in the Earth's gravity field. In this study, we have utilized various datasets to comprehend subsurface density variations and provide insights into the geodynamic prospects beneath the Western Ghats.

4.1. Topographic Map

The WPCM of India forms an uninterrupted coastal wall that spans from 8° to 22° N in latitude. It stretches over a length of approximately 1600 km, extending from the Tapti River in the north to Kanyakumari in the south. The only interruption in this expanse occurs in the Palakkad region near the southernmost part of India, where it narrows to roughly 30 km in width. This study used from the Shuttle Radar Topography Mission (SRTM) 15+ for topographic analysis [65]. The topography map (Fig. **1b**) depicts all major geological formations and exhibits a strong correlation with the regional geology (Fig. **1a**) in the study area. In the coastal region gradually ascends in a step-like pattern, marked by significant elevation changes. The topographic variations range from a minimum of -3.70 km to a maximum of 2.60 km. High topographic values are predominantly concentrated along the escarpment, while the oceanic region exhibits the lowest values. In particular, the southern part of the WDC and the northern section of the SGT feature prominently elevated topography, with the maximum elevation reaching 2.6 km in the Nilgiri block. In contrast, the EDC exhibits a flatter topography, averaging around 0.3 km, in comparison to other regions such as the DVP, WDC, CB, and SGT.

4.2. Complete Bouguer Anomaly Map

In the present study region, research efforts have been limited due to the challenging terrain characterized by hilly landscapes and a lack of accessible roads. This has posed significant logistical challenges for conducting on-site investigations. As a result, we have utilized satellite-based measurements derived from the Earth Gravitational Model (2008) to overcome these limitations and gain insights into crustal and lithospheric variations across the Western Ghats. The EGM2008 model [66] is a spherical harmonic model, which is obtained from satellite missions, including CHAMP and GRACE [66]. This model is freely accessible and contains coefficients extended up to a degree of 2190 with an order of 2159. The gravity method measures changes in the earth’s gravitational field on the earth’s surface to determine the subsurface lateral density variations, providing valuable indirect information on the mass distribution at depths.

The Complete Bouguer Anomaly (CBA) map, which has been terrain corrected to account for the influence of topography, is shown in Fig. (**1c**). This map provides a visual representation of gravity values ranging from -124 to 168 mGal. Gravity anomalies, both positive and negative, are depicted across the study area, offering insights into the subsurface density variations and mass distribution beneath the Earth's surface. Positive anomalies are predominantly observed in the oceanic and coastal plain regions, indicating areas with relatively higher mass concentrations beneath the Earth's surface. Conversely, negative anomalies are more prevalent in continental regions, with the largest negative anomalies observed in the western continental parts of the DVP, WDC, SGT, and CB. These negative anomalies are often associated with the presence of thick crustal roots. Remarkably, over the WPCM, we observe a distinct negative anomaly, especially in the NNW-SSE direction within the WDC. This region exhibits the lowest gravity anomalies, ranging from -124 to -35 mGal. Notably, this anomaly pattern closely correlates with the topography map (Fig. **1b**), where the areas of low gravity anomalies align with the elevated topographic features along the WPCM.

5. Radially Averaged Power Spectral Analyses

Radially Averaged Power Spectral Analysis is a commonly used statistical method for interpreting gravity and magnetic anomalies [67] to calculate the average depth of interface layers caused by subsurface sources. In this study, we applied 2-D Fourier Transformation analysis to the Complete Bouguer Anomaly (CBA) to distinguish

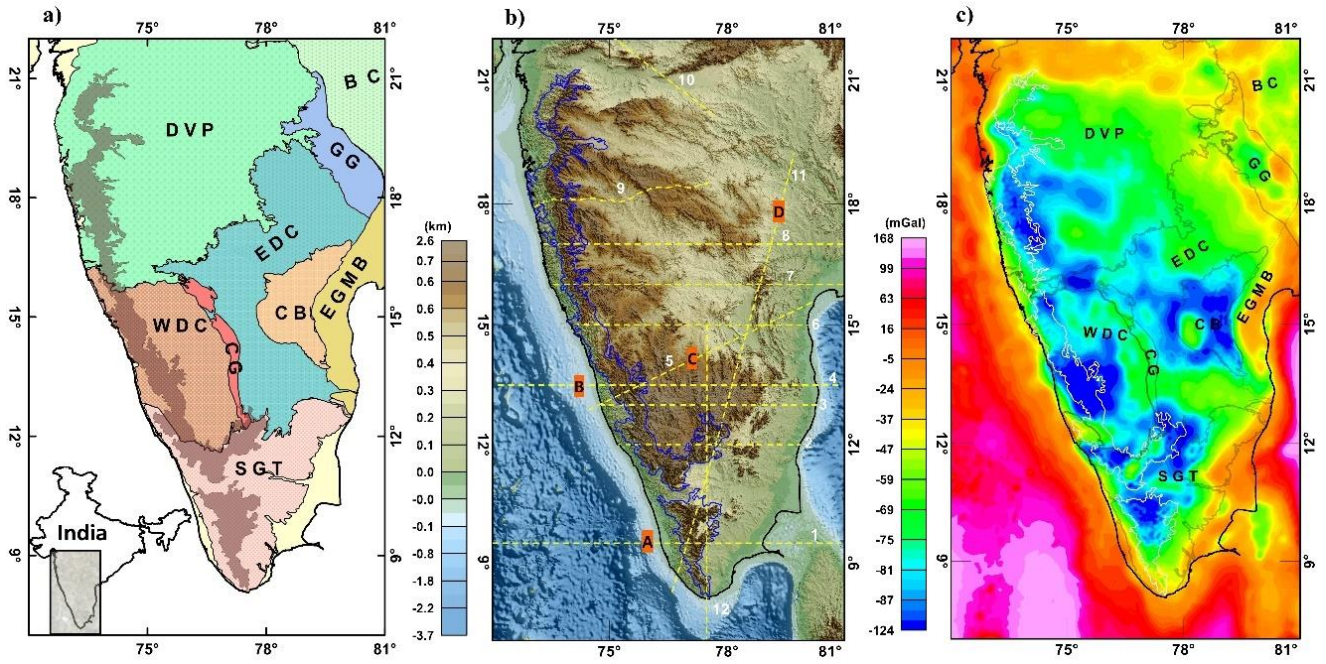

Figure 1: a) Regional geology map of the study area (after, Geological Survey of India, 1995). SGT: Southern granulite terrane, WDC: Western Dharwar Craton, CB: Cuddapah Basin, EDC: Eastern Dharwar Craton, EGMB: Eastern Ghat Mobile Belt, GG: Godavari Graben, DVP: Deccan Volcanic Province, BC: Bastar Craton, CG: Closepet Granite. Geology and tectonic map of study area shown grey coloured in rectangular box. **b**) Topography map of the study area (in km). The dashed yellow lines indicate previous gravity studies from various authors, the blue solid line represent escarpment. The references with red-colored backgrounds labeled as (A, B, C, D) have been selected to estimate the uncertainties in crust and lithospheric thickness. **c**) Complete Bouguer anomaly (in mGal) map.

between long-wavelength and short-wavelength signals associated with deeper and shallower sources, respectively. The CBA power spectrum plot, with wavenumber on the x-axis and the logarithm of spectral energy on the y-axis, shows a continuous decrease with increasing wavenumber. The gradient of the linear segments in the Fourier power spectrum is related to the average depth of various subsurface layers. Using the slopes of these lines, we calculated mean depths for the interface boundaries, which are denoted as L1= 176 km (LAB), L2= 47 km (Moho), L3= 21 km (Middle crust), and L4= 10 km (Upper crust) (Fig. **2**).

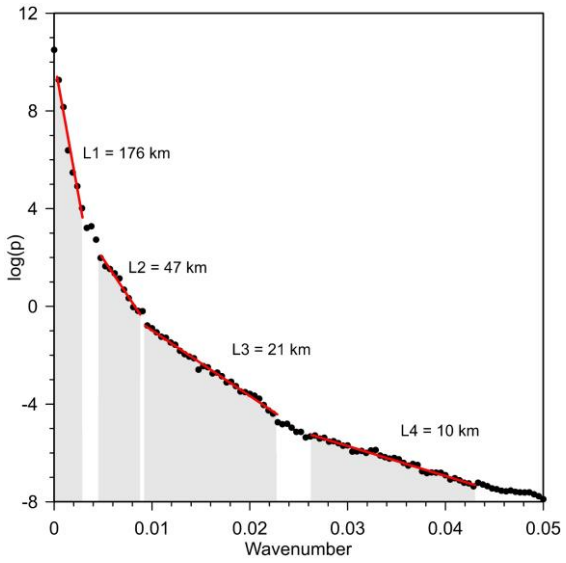

Figure 2: Radially averaged power spectrum calculated averaged depth to sources Complete Bouguer anomaly estimated different layers depths shown red colours. L1= 176 km (LAB), L2= 47 km (Moho), L3= 21 km (Middle crust), and L4= 10 km (Upper crust).

6. Uncertainties in Crust and Lithospheric Thickness

Many geophysical methods are non-unique, as they utilize various physical parameters to gain insights into and investigate the Earth's subsurface. The challenge lies in producing reliable geological images, primarily due to the limited data sources available on the Earth's surface, including deep seismic sounding, potential field data, receiver functions, and seismic tomography. Consequently, uncertainties arise during the interpretation of geophysical data, making it challenging to reach definitive conclusions. In this study, we interpreted a total of 12 profiles based on previous research results, incorporating a diverse set of gravity and magnetic anomalies, along with global models. Our objective was to estimate uncertainties in both crustal and lithospheric thickness. We employed the following formula to calculate these uncertainties:

$$\text{Uncertainty formula} = \sqrt{[\sum(x_i - \mu)^2/(n \times (n-1))]}$$

In this formula, x_i represents individual data points, μ is the mean, and n is the number of data points.

- The West-East-oriented profile (Fig. **3a**) along the 9.5°N latitude, which spans approximately 1000 km across the Arabian Sea, SGT, and the Bay of Bengal, clearly reveals positive gravity anomalies over the ocean and negative anomalies in the continental region. While the geoid anomaly does not exhibit a strong correlation in the western ocean part, it does align well with elevated areas. Regional gravity and isostatic anomalies indicate positive signatures, suggesting a shallower crustal and lithospheric depth, whereas negative anomalies imply thicker structures. According to [68], who used an integrated modeling approach, the Moho (crust-mantle boundary) and LAB (Lithosphere-Asthenosphere Boundary) depths are estimated to be around 12-15 km over the ocean and 27-36 km beneath the SGT. This depth range closely matches the findings of [69] in their global model (75%), but it deviates significantly from other global models and receiver function results, which display substantial variation. The LAB depth beneath the ocean ranges from 67 to 128 km, while it's approximately 130 km under the SGT, and these values do not align with any existing models. The maximum observed uncertainties in crustal and lithospheric thickness along this profile are 7.75 km and 18.79 km, respectively, with average estimated uncertainties in the crust and lithospheric variations at 13.04% and 23.92%.
- In another West-East profile (Fig. **3b**) along the 13.5°N latitude, the gravity anomaly exhibits a continuous decrease from west to east, except at the end of the profile, closely mirroring the variations in Moho and LAB depths. The Moho values obtained from [26] align closely with the trends observed in two global models, Crust1.0 and [69], but only match more than 85% with receiver function results over the WDC, CG, and EDC regions. The LAB depths observed beneath the WDC and EGMB indicate thickness, while those beneath CG and EDC appear thinner, deviating from the patterns seen in global models. The maximum observed uncertainties in crustal and lithospheric thickness along this profile are 5.86 km and 18.67 km, respectively, with average estimated uncertainties in the crust and lithospheric variations at 20.01% and 21.80%.
- Vasanthi and Santosh [70] estimated lithospheric structure based on satellite-derived gravity data (Fig. **3c**). Their results, obtained using the finite element technique, revealed clear demarcations of the boundaries of major geotectonic formations in the Dharwar craton, including the western, central, and eastern regions, as well as the surrounding areas. The averaged depths of the Moho and LAB beneath the various major blocks within the Dharwar craton were as follows: 38 km and 138-175 km for the western block, 41 km and 102-138 km for the central block, and 42 km and 88-120 km for the eastern block, respectively. At the boundaries between the western and central blocks, the depths were approximately 52 km and 147 km, while between the central and eastern blocks, they were around 46 km and 103 km. Notably, the results of this study did not align with any global models or receiver function analysis. The maximum observed uncertainties in the crust and lithospheric thickness along this profile were 7.85 km and 21.26 km, respectively. The average estimated uncertainties in the crust and variations in lithospheric thickness were 7.82% and 12.85%, respectively.
- A 1300 km-long profile in the SSW-NNE direction (Fig. **3d**) traverses the SGT, WDC, and Cuddapah basin, revealing numerous gravity and magnetic anomalies, including highs and lows. The crustal thickness, as estimated by [71] Kumar *et al*. (2020) using 2-D lithospheric density modeling, shows variations. It measures

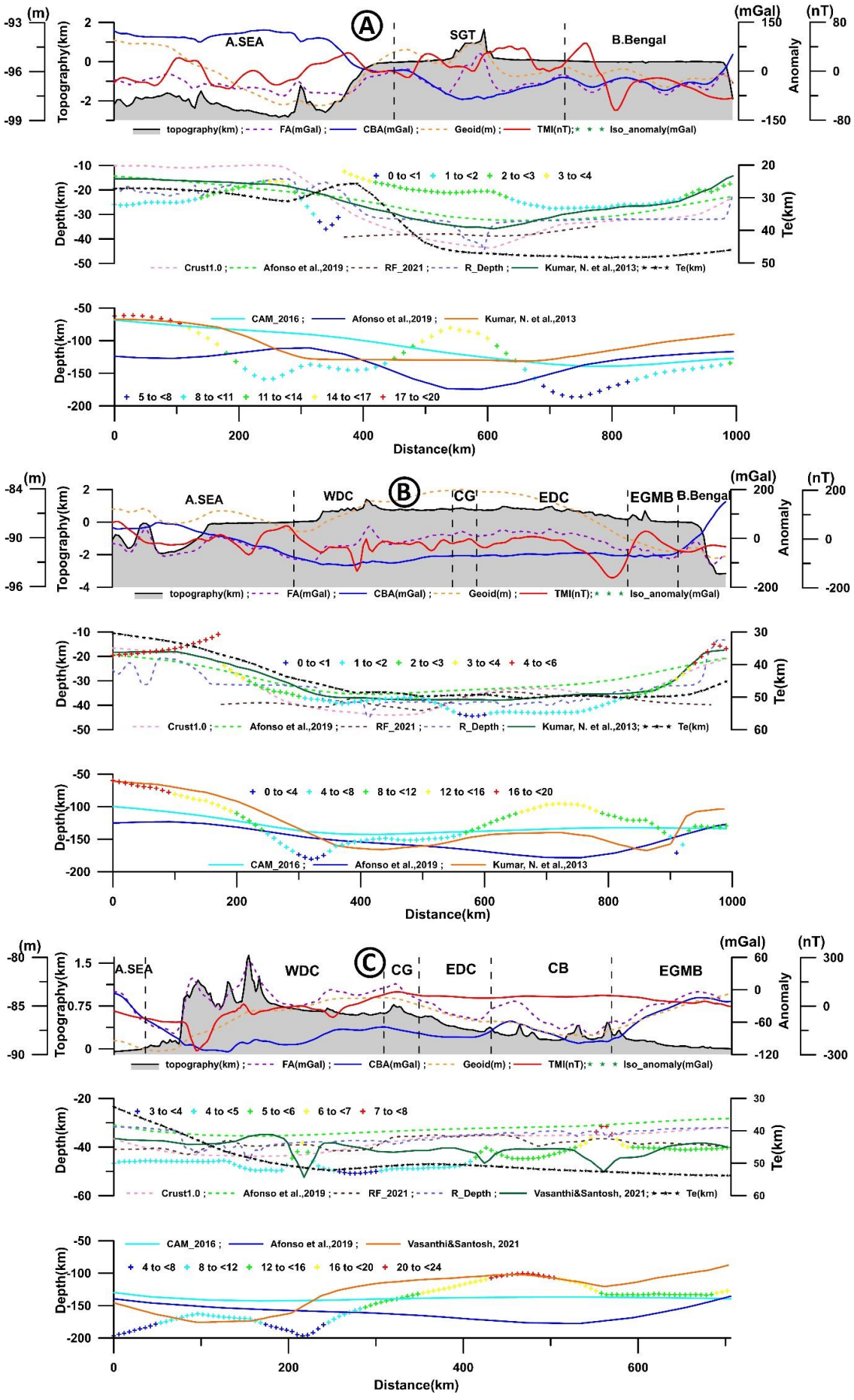
A
A.SEA
SGT
B.Bengal
(m)
(mGal)
(nT)
Topography(km)
Anomaly
topography(km) ; FA(mGal) ; CBA(mGal) ; Geoid(m) ; TMI(nT); Iso_anomaly(mGal)
Depth(km)
Te(km)
0 to <1
1 to <2
2 to <3
3 to <4
Crust1.0 ; Afonso et al.,2019 ; RF_2021 ; R_Depth ; Kumar, N. et al.,2013; Te(km)
CAM_2016 ; Afonso et al.,2019 ; Kumar, N. et al.,2013
5 to <8
8 to <11
11 to <14
14 to <17
17 to <20
Distance(km)
B
A.SEA
WDC
CG
EDC
EGMB
B.Bengal
4 to <6
C
A.SEA
WDC
CG
EDC
CB
EGMB
Vasanthi&Santosh, 2021; Te(km)
Vasanthi&Santosh, 2021
4 to <8
8 to <12
12 to <16
16 to <20
20 to <24

(Figure 3) contd....

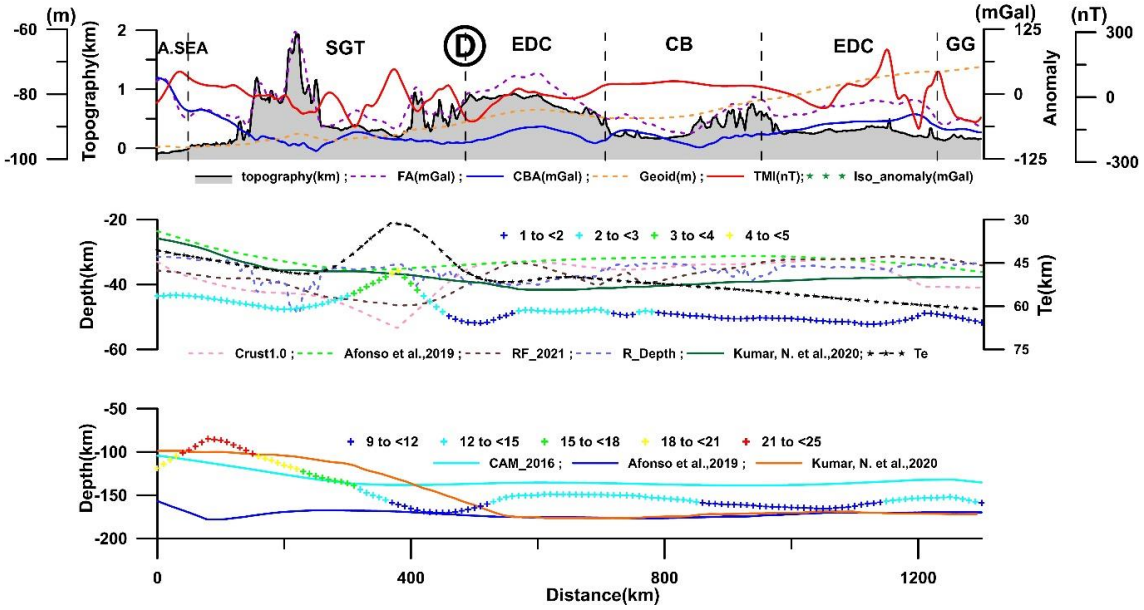

Figure 3: Uncertainty analysis estimated maps from Previous studies correlation with available global and receiver functions results. **A**) Profile no.1 showing the yellow dot lines in (Fig. **1b**) taken from Kumar et al., 2013. **B**) Profile no. 4 showing the yellow dot lines in (Fig. **1b**) taken from Kumar et al., 2013. **C**) Profile no.5 showing the yellow dot lines in (Fig. **1b**) taken from Vasanthi and Santosh, 2021. **D**) Profile no.11 showing the yellow dot lines in (Fig. **1b**) taken from Kumar et al., 2019. SGT: Southern granulite terrane, WDC: Western Dharwar Craton, CB: Cuddapah Basin, EDC: Eastern Dharwar Craton, EGMB: Eastern Ghat Mobile Belt, GG: Godavari Graben, CG: Closepet Granite.

approximately 25 km in the ocean, around 41 km under the SGT, and between 38-40 km in the WDC and Cuddapah basin regions. The calculated lithospheric thickness exhibits variations beneath the SGT and Eastern Indian shield, measuring between 120-130 km. In contrast, the WDC region displays a lithospheric thickness of 160-180 km. These values do not correlate with global models or receiver function data. The maximum observed uncertainties in the crust and lithospheric thickness along this profile are 4.27 km and 24.18 km, respectively. The average estimated uncertainties for crust and lithospheric variations are 18.47% and 14.26%, respectively.

7. 2-D Lithospheric Density Modeling along the Western Ghat Escarpment

Furthermore, we conducted 2-D lithospheric density modeling along the Western Ghat Escarpment (WPCM). This involved generating cross-sections along three lengthy profiles, each spanning approximately 1600 km and oriented in the SSE-NNW direction. These profiles, labeled as A-A', B-B', and C-C' (Fig. **4a**), traverse various lithological blocks within the region, including the SGT, WDC, and DVP.To perform this modeling, we utilized Geosoft GM-SYS software, originally developed for potential fields by [72, 73]. It enabled us to perform forward modeling effectively. In a Cartesian coordinate system, the gravity anomaly profile of a 2-D anomalous density source in a plane perpendicular to the strike (in the y-directional extension) can be approximated using a polygon [72]. Improving the accuracy of this geometric representation involves increasing the number of vertices in the polygon. According to [72], The vertical component of the gravity field anomaly (g_z) at point P (xi, zi) due to an infinitely extending mass source with a density contrast ($\Delta\rho$) in the y-direction can be expressed as:

$$g_z(x_i, z_i) = 2G \iint_S \frac{\Delta\rho \,.\, (z - z_i)}{(x - x_i)^2 + (z - z_i)^2}\, dx\, dz$$

Where G is the universal gravitational constant.

It's important to note that interpreting potential data modeling often encounters non-uniqueness challenges. This is primarily due to the lack of direct information related to subsurface structures, petrophysical

characteristics, and the composition of various crustal and lithospheric layers. Given this complexity, it's possible to create an infinite number of models that produce the same observed gravity anomaly. To address this ambiguity, we employ a strategy of constraining the model using previously acquired complementary information.

In our approach, we have incorporated available seismic constraints obtained from receiver functions in various studies to determine both crustal thickness and the depth of the LAB. These constraints have been drawn from a range of sources, including gravity studies with seismic constraints [74], converted wave techniques such as P and S receiver functions [60], 2-D lithospheric density modeling developed by [68], a 3-D lithospheric model established using surface wave observations and classical tomographic methods [61], as well as a finite element approach applied by [70]. The initial depths of the model's layers have been derived from radially averaged power spectrum analysis (Fig. **2**).

7.1. Profile – A-A’

The western section of this profile has been specifically chosen along the coastal area, characterized by a range of gravity anomalies, with values fluctuating between -55 mGal and 41 mGal. The most notable positive gravity anomalies have been observed beneath the DVP, reaching approximately 40 mGal. The gravity model, constrained by seismic data and applied along this profile, provides insights into crustal thickness variations. Within this model, the SGT region displays a crustal thickness ranging from 33 km to 42 km, the WDC region ranges from 39 km to 42 km, and the DVP region exhibits variability from 31 km to 43 km (Fig. **4b**). Likewise, the LAB's variation is evident in the SGT region, spanning from 57 km to 83 km, in the WDC region, ranging from 76 km to 80 km, and in the DVP region, extending from 79 km to 94 km.

7.2. Profile – B-B’

Profile B-B' has been precisely positioned over the escarpment, exhibiting the most significant negative Bouguer anomaly compared to the other profiles. The range of anomalies varies from a minimum of -118 mGal to a maximum of -37 mGal. Two noteworthy features stand out in this profile. First, near the geological boundary between SGT and WDC, there is a wavelength of approximately 200 km with a fluctuating anomaly of around -60 mGal. Second, near the boundary between EDC and DVP, there is a wavelength of approximately 175 km with a fluctuating anomaly of about 35 mGal. Crustal thickness estimates have been determined based on constrained seismic results, revealing values for SGT ranging from 34 km to 45 km, WDC ranging from 37 km to 48 km, and DVP ranging from 34 km to 42 km. Additionally, LAB variations have been estimated within the Western Ghat, with constrained data available from select locations within the major geological blocks. These estimates indicate depths for SGT ranging from 87 km to 160 km, WDC ranging from 137 km to 166 km, and DVP ranging from 92 km to 137 km (Fig. **4c**). Notably, a thick LAB, measuring between 150 km and 166 km, has been observed beneath the northern part of SGT and the southern part of WDC, corresponding to a highly elevated region.

7.3. Profile – C-C’

This profile has been chosen on the eastern side of the uplifted escarpment, revealing numerous undulations in gravity anomalies. The topographic variations are largely linear, spanning approximately 750 meters, except at the boundaries between SGT and WDC. The gravity anomaly along the profile exhibits an overall range from -97 mGal to +6 mGal, encompassing three major geological units. We have determined variations in the crustal structure beneath these units, with SGT ranging from 36 km to 47 km, WDC from 42 km to 46 km, and DVP from 36 km to 42 km. Regarding the depth of the LAB, we observe depths of 114 km to 142 km in SGT, 115 km to 148 km in WDC, and 82 km to 115 km in DVP. Notably, most of the SGT and the southern parts of WDC display similar crustal and lithospheric variations, approximately measuring 45 km and 140 km, respectively (Fig. **4d**).

8. Conclusion

The accurate characterization of the subsurface of geological structures primarily relies on geoscientific input data. Nevertheless, uncertainties within this input data have the potential to yield unreliable geological structures, thereby affecting the reliability of geoscientific findings. In this study, we present several profiles depicting variations

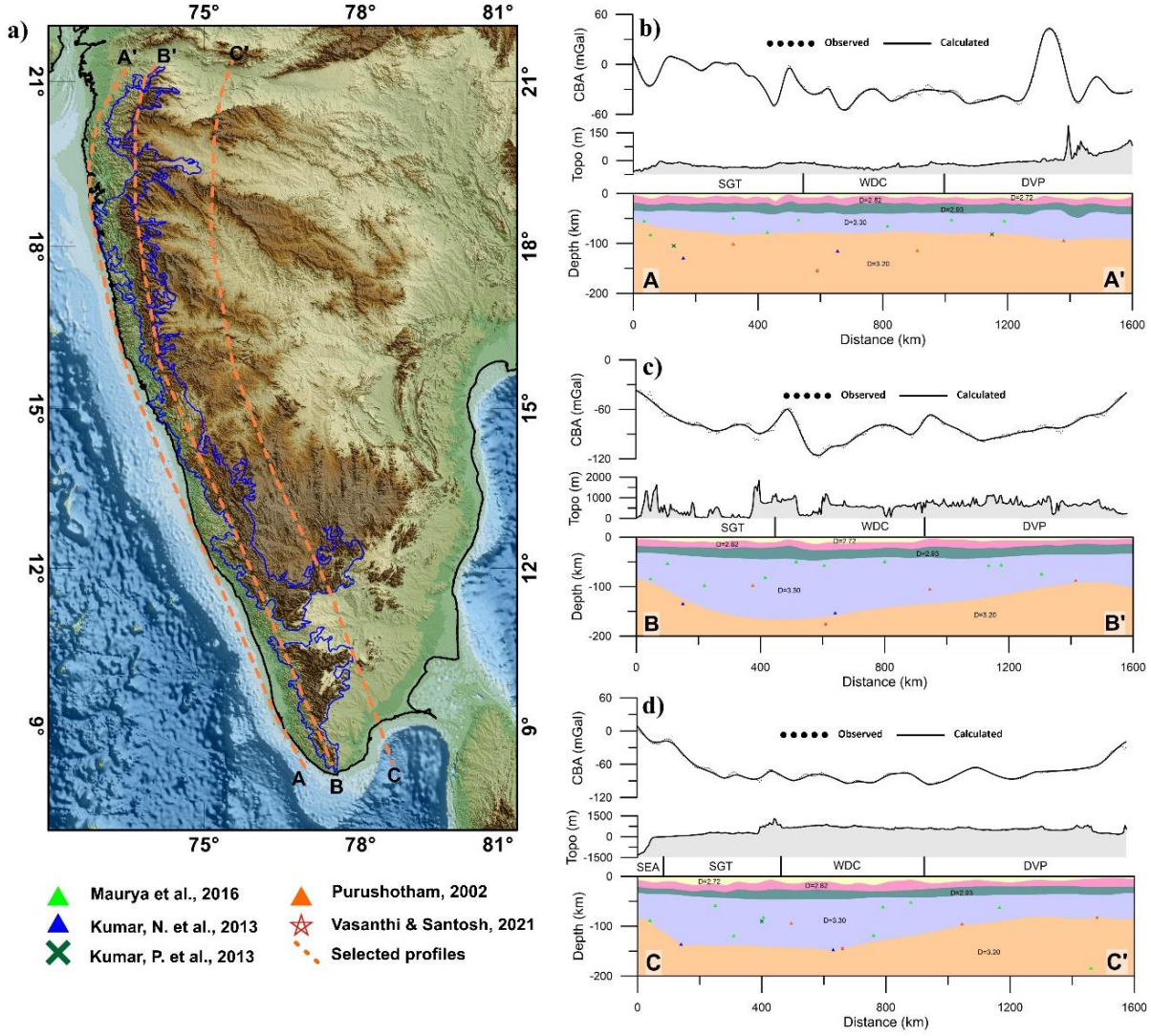

Figure 4: 2D density lithospheric modelling **a**) Topography map of the study area, dashed orange lines indicate selected three (A-A', B-B', C-C') SSE to NNW profiles. The solid blue line is representing the Western ghat's escarpment **b**) Profile A-A' profile selected western part of the escarpment **c**) Profile B-B' profile selected over the escarpment d) Profile C-C' profile selected eastern side of the escarpment. The major geological boundaries shown by thick vertical black solid lines. D: Density, SGT: Southern granulite terrane, WDC: Western Dharwar Craton, EDC: Eastern Dharwar Craton, DVP: Deccan Volcanic Province.

in crustal and lithospheric thickness that exhibit significant differences from one another. These variations in crustal and lithospheric thickness range from 8% to 20% and 13% to 24%, respectively. Such disparities can exert a profound influence on tectonic and geodynamic interpretations. Our research encompasses the Western Ghats and the surrounding regions of SGT, WDC, and DVP, characterized by distinct structural and physical properties. The precise mechanisms governing the evolution of the Western Ghats and its connection with the maturation of the Western Ghat Coastal Margin (WPCM) remain enigmatic. Therefore, we have undertaken 2-D lithospheric density modeling of crustal and lithospheric structures along the Western Ghat escarpment, utilizing three selected profiles. These profiles have been constrained by previous geophysical studies and globally available models. The density model unveils a five-layered configuration, providing insights into crustal thickness over SGT (ranging from 33 km to 47 km), WDC (ranging from 37 km to 48 km), and DVP (ranging from 31 km to 43 km). The lithospheric-asthenospheric boundary depths vary in SGT (ranging from 57 km to 160 km), WDC (ranging from 76 km to 166 km), and DVP (ranging from 79 km to 137 km). The conspicuous changes in crustal and lithospheric structures along the Western Ghats escarpment hint at distinct tectonic and drifting episodes along the western margin of India. Further investigations are required to validate this concept and reduce uncertainties, contributing to a better understanding of the tectonic evolution of India's Passive Continental Margin.

Conflict of Interest

We declare that we have no commercial or affiliative interests that could pose a conflict of interest concerning the work presented.

Acknowledgments

We sincerely acknowledge the Ministry of Earth Sciences, Government of India for supporting this project under the core program of the National Centre for Earth Science Studies (NCESS), India. The authors are also thankful to the Director, NCESS, Thiruvananthapuram, for his permission to publish this article. We extend our gratitude to Dr. Mehmet Sari, Co-Editor-in-Chief, as well as two anonymous reviewers, for their valuable and thoughtful comments on the manuscript. Their insights have significantly contributed to the enhancement of our results and the overall quality of the manuscript.

References

[1] Yuan H, Romanowicz B. Introduction-lithospheric discontinuities, John Wiley & Sons; 2019, p. 1-3. https://doi.org/10.1002/9781119249740.ch0

[2] Kale VS. The western ghat: the great escarpment of India. In: Migon P, Ed., Geomorphological Landscapes of the World, Dordrecht: Springer; 2009, p. 257-64. https://doi.org/10.1007/978-90-481-3055-9_26

[3] Weissel JK, Karner GD. Flexural uplift of rift flanks due to mechanical unloading of the lithosphere during extension. J Geophys Res Solid Earth. 1989; 94: 13919-50. https://doi.org/10.1029/JB094iB10p13919

[4] Radhakrishna BP. Neogene uplift and geomorphic rejuvenation of the Indian Peninsula. Curr Sci. 1993; 64: 787-93.

[5] Matmon A, Bierman P, Enzel Y. Pattern and tempo of great escarpment erosion. Geology. 2002; 30: 1135-8. https://doi.org/10.1130/0091-7613(2002)030<1135:PATOGE>2.0.CO;2

[6] Campbell IH, Griffiths RW. Implications of mantle plume structure for the evolution of flood basalts. Earth Planet Sci Lett. 1990; 99: 79-93. https://doi.org/10.1016/0012-821X(90)90072-6

[7] Gunnell Y, Harbor D. Structural underprint and tectonic overprint in the Angavo (Madagascar) and Western Ghats (India) - Implications for understanding scarp evolution at passive margins. J Geol Soc India. 2008; 71: 763-79.

[8] Devey CW, Lightfoot PC. Volcanological and tectonic control of stratigraphy and structure in the western Deccan traps. Bull Volcanol. 1986; 48: 195-207. https://doi.org/10.1007/BF01087674

[9] Tiwari VM, Vyaghreswara Rao MBS, Mishra DC. Density inhomogeneities beneath Deccan Volcanic Province, India as derived from gravity data. J Geodyn. 2001; 31: 1-17. https://doi.org/10.1016/S0264-3707(00)00015-6

[10] McKenzie D. Some remarks on the development of sedimentary basins. Earth Planet Sci Lett. 1978; 40: 25-32. https://doi.org/10.1016/0012-821X(78)90071-7

[11] Gunnell Y, Fleitout L. Morphotectonic evolution of the western ghats, India. In: Summerfield MA, Ed., Geomorphology and Global Tectonics. Vol. 23, Wiley; 2000, p. 321-36.

[12] Gunnell Y, Radhakrishna BP. The Great Escarpment of the Indian Subcontinent (Patterns of Landscape Development in the Western Ghats). Bangalore: Geological Society of India; 2001, p. 1053.

[13] Widdowson M, Cox KG. Uplift and erosional history of the Deccan Traps, India: Evidence from laterites and drainage patterns of the Western Ghats and Konkan Coast. Earth Planet Sci Lett. 1996; 137: 57-69. https://doi.org/10.1016/0012-821X(95)00211-T

[14] Cockburn HAP, Brown RW, Summerfield MA, Seidl MA. Quantifying passive margin denudation and landscape development using a combined fission-track thermochronology and cosmogenic isotope analysis approach. Earth Planet Sci Lett. 2000; 179: 429-35. https://doi.org/10.1016/S0012-821X(00)00144-8

[15] Brown R, Cockburn H, Kohn B, Belton D, Fink D, Gleadow A, et al. Combining low temperature apatite thermochronology and cosmogenic isotope analysis in quantitative landscape evolution studies. Geochim Cosmochim Acta. 2002; 66: A106.

[16] van der Beek P, Summerfield MA, Braun J, Brown RW, Fleming A. Modeling postbreakup landscape development and denudational history across the southeast African (Drakensberg Escarpment) margin. Curr Sci. 2001; 107: 1-18. https://doi.org/10.1029/2001JB000744

[17] Gunnell Y, Gallagher K, Carter A, Widdowson M, Hurford AJ. Denudation history of the continental margin of western peninsular India since the early Mesozoic – reconciling apatite fission-track data with geomorphology. Earth Planet Sci Lett. 2003; 215: 187-201. https://doi.org/10.1016/S0012-821X(03)00380-7

[18] Persano C, Stuart FM, Bishop P, Dempster TJ. Deciphering continental breakup in eastern Australia using low-temperature thermochronometers. J Geophys Res Solid Earth. 2005; 110: 1-17. https://doi.org/10.1029/2004JB003325

[19] Gilchrist AR, Summerfield MA. Differential denudation and flexural isostasy in formation of rifted-margin upwarps. Nature. 1990; 346: 739-42. https://doi.org/10.1038/346739a0

[20] Gilchrist AR, Summerfield MA. Tectonic models of passive margin evolution and their implications for theories of long-term landscape development. In: Kirkby MJ, Ed., Process Models and Theoretical Geomorphology. Chichester: 1994, p. 55-84.

[21] Valdiya KS. Tectonic resurgence of the Mysore plateau and surrounding regions in cratonic Southern India. Curr Sci. 2001; 81: 1068–89.

[22] Gunnell Y. Dynamics and kinematics of rifting and uplift at the western continental margin of India, Insights from geophysics and numerical models. Sahyadri, the great escarpment of the Indian subcontinent. Geol Soc India Mem. 2001; 47: 475–96

[23] Mandal B, Vijaya Rao V, Karuppannan P, Laxminarayana K. Mechanism for epeirogenic uplift of the archean Dharwar craton, southern India as evidenced by orthogonal seismic reflection profiles. Sci Rep. 2021; 11: Article number: 1499. https://doi.org/10.1038/s41598-021-80965-7

[24] Radhakrishna T, Mohamed AR, Venkateshwarlu M, Soumya GS, Prachiti PK. Mechanism of rift flank uplift and escarpment formation evidenced by Western Ghats, India. Sci Rep. 2019; 9: Article number: 10511. https://doi.org/10.1038/s41598-019-46564-3

[25] Dubey CP, Tiwari VM. Gravity anomalies and crustal thickness variations over the western ghats. J Geol Soc India. 2018; 92: 517-22. https://doi.org/10.1007/s12594-018-1059-7

[26] Gupta S, Kanna N, Kumar S, Sivaram K. Crustal thickness and composition variation along the western ghats of India through teleseismic receiver function analysis. J Geol Soc India. 2018; 92: 523-8. https://doi.org/10.1007/s12594-018-1061-0

[27] Sinha-Roy S. A hybrid multistage model of evolution of the Western Ghats at the passive western continental margin of India. J Geol Soc India. 2018; 92: 533–41. https://doi.org/10.1007/s12594-018-1063-y

[28] Sribin C, Padma Rao B, Ravi Kumar M, Tomson JK. Mantle deformation beneath the Western Ghats, India: Insights from core-refracted shear wave splitting analysis. J Asian Earth Sci. 2021; 218: 104848. https://doi.org/10.1016/j.jseaes.2021.104848

[29] B PR, M RK. Evolution of the Western Ghats: Constraints from receiver function imaging and harmonic decomposition. Tectonophysics. 2022; 838: 229472. https://doi.org/10.1016/j.tecto.2022.229472

[30] Moore A, Blenkinsop T, Cotterill F. Southern African topography and erosion history: plumes or plate tectonics? Terra Nova. 2009; 21: 310–5. https://doi.org/10.1111/j.1365-3121.2009.00887.x

[31] Osmundsen PT, Redfield TF. Crustal taper and topography at passive continental margins. Terra Nova. 2011; 23: 349-61. https://doi.org/10.1111/j.1365-3121.2011.01014.x

[32] Singh AP, Kumar N, Prabhakar Rao MRK, Singh B. Crustal configuration beneath the Palghat gap (South India) and mantle-crust connections. In: Satake K, Ed. Advances in Geosciences. Singapore: World Scientific; 2011, p. 117-29. (Solid Earth; Vol. 26).

[33] Besse J, Courtillot V. Revised and synthetic apparent polar wander paths of the African, Eurasian, North American and Indian plates, and true polar wander since 200 Ma. J Geophys Res Solid Earth. 1991; 96: 4029-50. https://doi.org/10.1029/90JB01916

[34] Storey BC. The role of mantle plumes in continental breakup: case histories from Gondwanaland. Nature. 1995; 377: 301-8. https://doi.org/10.1038/377301a0

[35] Veevers JJ. Gondwanaland from 650–500 Ma assembly through 320 Ma merger in Pangea to 185–100 Ma breakup: supercontinental tectonics via stratigraphy and radiometric dating. Earth Sci Rev. 2004; 68: 1-132. https://doi.org/10.1016/j.earscirev.2004.05.002

[36] Caxito F de A, Alkmim FF. The role of V-shaped oceans and ribbon continents in the brasiliano/panAfrican assembly of western Gondwana. Sci Rep. 2023; 13: Article number: 1568. https://doi.org/10.1038/s41598-023-28717-7

[37] Richetti PC, Schmitt RS, Reeves C. Dividing the South American continent to fit a Gondwana reconstruction: A model based on continental geology. Tectonophysics. 2018; (747-748): 79-98. https://doi.org/10.1016/j.tecto.2018.09.011

[38] Raval U, Veeraswamy K. India-Madagascar separation: breakup along a pre-existing mobile belt and chipping of the craton. Gondwana Res. 2003; 6: 467-85. https://doi.org/10.1016/S1342-937X(05)70999-0

[39] Reeves C. The position of Madagascar within Gondwana and its movements during Gondwana dispersal. J Afr Earth Sci. 2014; 94: 45–57. https://doi.org/10.1016/j.jafrearsci.2013.07.011

[40] White R, McKenzie D. Magmatism at rift zones: The generation of volcanic continental margins and flood basalts. J Geophys Res Solid Earth. 1989; 94: 7685-729. https://doi.org/10.1029/JB094iB06p07685

[41] Behera L, Sen MK. Tomographic imaging of sub-basalt mesozoic sediments and shallow basement geometry for hydrocarbon potential below the Deccan Volcanic Province (DVP) of India. Geophys J Int. 2014; 199: 296-314. https://doi.org/10.1093/gji/ggu261

[42] Beckinsale RD, Drury SA, Holt RW. 3,360-Myr old gneisses from the south Indian craton. Nature. 1980; 283: 469-70. https://doi.org/10.1038/283469a0

[43] Talukdar M, Sarkar T, Sengupta P, Mukhopadhyay D. The Southern Granulite Terrane, India: The saga of over 2 billion years of Earth's history. Earth Sci Rev. 2022; 232: 104157. https://doi.org/10.1016/j.earscirev.2022.104157

[44] Tewari HC, Kumar P. Lithospheric framework of the Indian sub-continent through Seismic and Seismological Studies. Episodes. 2020; 43: 622-37. https://doi.org/10.18814/epiiugs/2020/020041

[45] Radhakrishna M, Kurian PJ, Nambiar CG, Murty BVS. Nature of the crust below the Southern Granulite Terrain (SGT) of Peninsular India across the Bavali shear zone based on analysis of gravity data. Precambrian Res. 2003; 124: 21-40. https://doi.org/10.1016/S0301-9268(03)00047-0

[46] Sunil PS, Radhakrishna M, Kurian PJ, Murty BVS, Subrahmanyam C, Nambiar CG, et al. Crustal structure of the western part of the Southern Granulite Terrain of Indian Peninsular Shield derived from gravity data. J Asian Earth Sci. 2010; 39: 551-64. https://doi.org/10.1016/j.jseaes.2010.04.028

[47] Lasitha S, Twinkle D, John Kurian P, Harikrishnan PR. Geophysical evidence for marine prolongation of the palghat-cauvery shear system into the offshore cauvery basin, eastern continental margin of India. J Asian Earth Sci. 2019; 184: 103981. https://doi.org/10.1016/j.jseaes.2019.103981

[48] Prasad M, Dubey CP, Joshi KB, Tiwari VM. Crustal density and susceptibility structure beneath Achankovil shear zone, India. Lithosphere. 2021; 2021: 6017801. https://doi.org/10.2113/2021/6017801

[49] Prasad M, Dubey CP. Tectonic and structural elements of Southern Granulite Terrane, South India: Inferences from gravity and magnetic studies. J Asian Earth Sci. 2023; 256: 105823. https://doi.org/10.1016/j.jseaes.2023.105823

[50] Rai SS, Ramesh DS. Seismic imaging of the Indian continental lithosphere. Proc India Sci Acad. 2012; 78: 353-9.

[51] Rai S, Borah K, Das R, Gupta S, Srivastava S, Prakasam KS, et al. The South India Precambrian crust and shallow lithospheric mantle: Initial results from the India Deep Earth Imaging Experiment (INDEX). J Earth System Sci. 2013; 122: 1435–53. https://doi.org/10.1007/s12040-013-0357-0

[52] Borah K, Rai SS, Gupta S, Prakasam KS, Kumar S, Sivaram K. Preserved and modified mid-archean crustal blocks in dharwar craton: Seismological evidence. Precambrian Res. 2014; 246: 16-34. https://doi.org/10.1016/j.precamres.2014.02.003

[53] Suresh G, Bhattacharya SN, Teotia SS. Crust and upper mantle velocity structure of the northwestern indian peninsular shield from inter-station phase velocities of Rayleigh and Love waves. Ann Geophys. 2015; 58: S0215. https://doi.org/10.4401/ag-6674

[54] Das R, Saikia U, Rai SS. The deep geology of south india inferred from moho depth and Vp/Vs ratio. Geophys J Int. 2015; 203: 910–26. https://doi.org/10.1093/gji/ggv351

[55] Das R, Rai SS. Redefining dharwar craton-southern granulite terrain boundary in south India from new seismological constraints. Precambrian Res. 2019; 332: 105394. https://doi.org/10.1016/j.precamres.2019.105394

[56] Gupta S, Rai SS, Prakasam KS, Srinagesh D, Bansal BK, Chadha RK, et al. The nature of the crust in southern India: Implications for precambrian crustal evolution. Geophys Res Lett. 2003; 30: 1419. https://doi.org/10.1029/2002GL016770

[57] Sarkar RK, Saha DK. A note on the lithosphere thickness and heat flow density of the Indian Craton from MAGSAT data. Acta Geophysica. 2006; 54: 198-204. https://doi.org/10.2478/s11600-006-0017-8

[58] Mitra S, Priestley K, Gaur V, Rai S. Shear-wave structure of the south Indian lithosphere from rayleigh wave phase-velocity measurement. Bull Seismol Soc Am. 2006; 96: 1551-9. https://doi.org/10.1785/0120050116

[59] Kumar P, Yuan X, Kumar MR, Kind R, Li X, Chadha RK. The rapid drift of the Indian tectonic plate. Nature. 2007; 449: 894-7. https://doi.org/10.1038/nature06214

[60] Kumar P, Kumar RM, Srijayanthi G, Arora K, Srinagesh D, Chadha RK, et al. Imaging the lithosphere-asthenosphere boundary of the Indian plate using converted wave techniques. J Geophys Res Solid Earth. 2013; 118: 5307-19. https://doi.org/10.1002/jgrb.50366

[61] Maurya S, Montagner JP, Kumar MR, Stutzmann E, Kiselev S, Burgos G, et al. Imaging the lithospheric structure beneath the Indian continent. J Geophys Res Solid Earth. 2016; 121: 7450-68. https://doi.org/10.1002/2016JB012948

[62] Kusham, Pratap A, Pradeep Naick B, Naganjaneyulu K. Lithospheric architecture in the Archaean Dharwar craton, India: A magnetotelluric model. J Asian Earth Sci. 2018; 163: 43-53. https://doi.org/10.1016/j.jseaes.2018.05.022

[63] Saha GK, Prakasam KS, Rai SS. Diversity in the peninsular Indian lithosphere revealed from ambient noise and earthquake tomography. Phys Earth Planet Inter. 2020; 306: 106523. https://doi.org/10.1016/j.pepi.2020.106523

[64] Mullick N, Rai SS, Saha G. Lithospheric structure of the South India Precambrian terrains from surface wave tomography. J Geophys Res Solid Earth. 2022; 127: e2022JB024244. https://doi.org/10.1029/2022JB024244

[65] Becker JJ, Sandwell DT, Smith WHF, Braud J, Binder B, Depner J, et al. Global bathymetry and elevation data at 30 arc seconds resolution: SRTM30_PLUS. Marine Geodesy. 2009; 32: 355-71. https://doi.org/10.1080/01490410903297766

[66] Pavlis NK, Holmes SA, Kenyon SC, Factor JK. The development and evaluation of the Earth Gravitational Model 2008 (EGM2008). J Geophys Res Solid Earth. 2012; 117: B04406. https://doi.org/10.1029/2011JB008916

[67] Spector A, Grant FS. Statistical models for interpreting aeromagnetic data. Geophysics. 1970; 35: 293-302. https://doi.org/10.1190/1.1440092

[68] Kumar N, Zeyen H, Singh AP, Singh B. Lithospheric structure of southern Indian shield and adjoining oceans: integrated modelling of topography, gravity, geoid and heat flow data. Geophys J Int. 2013; 194: 30-44. https://doi.org/10.1093/gji/ggt080

[69] Afonso JC, Salajegheh F, Szwillus W, Ebbing J, Gaina C. A global reference model of the lithosphere and upper mantle from joint inversion and analysis of multiple data sets. Geophys J Int. 2019; 217: 1602-28. https://doi.org/10.1093/gji/ggz094

[70] Vasanthi A, Santosh M. Lithospheric architecture and geodynamics of the Archean Dharwar craton and surrounding terranes: New insights from satellite gravity investigation. Gondwana Res. 2021; 95: 14-28. https://doi.org/10.1016/j.gr.2021.03.008

[71] Kumar N, Singh AP, Tiwari VM. Gravity anomalies, isostasy and density structure of the Indian continental lithosphere. Episodes. 2020; 43: 609-21. https://doi.org/10.18814/epiiugs/2020/020040

[72] Talwani M, Worzel JL, Landisman M. Rapid gravity computations for two-dimensional bodies with application to the Mendocino submarine fracture zone. J Geophys Res. 1959; 64: 49-59. https://doi.org/10.1029/JZ064i001p00049

[73] Talwani M, Heirtzler J, Parks G. Computation of magnetic anomalies caused by two dimensional bodies of arbitrary shape. In: Parks GA, Ed. Computers in the Mineral Industries, Part 1. 1964; CA: Stanford University Press; pp. 464-80. (Geological Sciences; Vol. 9).

[74] Purushotham AK. Geophysical constraints on structure and tectonics of the eastern arabian sea and the adjoining west coast of india with special reference to the kerala basin (Doctoral dissertation). School of Marine Sciences; 2002.